Ion−Molecule Reaction Mechanism of $SiCN^+/SiNC^+ + HX$ (X = H, CH_3, F, OH, NH_2)

Jian Wang, Yi-hong Ding,* and Chia-chung Sun

State Key Laboratory of Theoretical and Computational Chemistry, Institute of Theoretical Chemistry, Jilin University, Changchun 130023, People's Republic of China

Received: February 20, 2005; In Final Form: April 21, 2005

In contrast to the abundant data on the neutral−neutral reactions, little is known about the ion−molecule reactions involving silicon ions. A detailed mechanistic study at the B3LYP/6-311G(d,p) and CCSD(T)/6-311+G(2df,p) (single-point) computational levels was reported for the reactions of $SiCN^+/SiNC^+$ with a series of σ-bonded molecules HX (X = H, CH_3, F, NH_2). Together with the recently studied $SiCN^+/SiNC^+ + H_2O$ reactions, all of these reactions have nucleophilic substitution as their major pathway. Insertion is a much slower reaction. By contrast, the known atomic Si^+ and C_2N^+ ion−molecule reactions go by insertion. Generally, the initial gas-phase condensation between $SiCN^+/SiNC^+$ and HX (except the nonionic H_2) effectively forms the adduct HX...$SiCN^+$/HX...$SiNC^+$. The stability of the adduct increases with the electron-donating ability of X. Even at low temperatures, reactions with the electron donors NH_3, H_2O, and HF proceed rapidly to generate the fragments SiX^+ + HCN (dominant) and SiX^+ + HNC (minor). This suggests that such reactions may be useful in the synthesis of novel Si−X bonded species. However, the reactions of $SiCN^+$ with completely saturated CH_4 and H_2 produce fragments only at high temperatures, and $SiNC^+$ may even be unreactive. The calculated results may be helpful for understanding the chemistry of SiCN-based microelectric and photoelectric processes in addition to astrophysical processes in which the $[Si,C,N]^+$ ion is involved. The results can also provide useful mechanistic information for the analogous ion−molecule reactions of the monovalent silicon-bearing ions.

1. Introduction

Gas-phase reactions involving silicon-containing ions are important in severral processes, for example, the fabrication of microelectric and photoelectric materials. The reactions of silicon-bearing ions with environmental gases or dopants (usually in minute amounts) such as H_2O and NH_3 are also of interest. Up to now, the ion−molecule chemistry of some smaller ionic species such as atomic Si^+ (with CH_4, NH_3, H_2O, H_2, HCl, H_2S, C_2H_6, C_2H_4, C_2H_2, C_6H_6, CH_2CCH_2, CH_3CCH, and C_4H_2),[1−7] SiH^+ (with NH_3),[8] and SiH_3^+ (with NH_3, C_2H_4)[9,10] have been studied experimentally. It has been found that these reactions produce a wide variety of silicon-bonded species. The kinetics of more complex silicon-related reactions has received little attention. Although neutral−neutral reactions involving Si-species have been extensively studied,[11−27] theoretical investigations for the reactions of Si-bearing ions are relatively few.[1,28] Usually, the reaction mechanism of silicon-bearing species has been considered to be similar to those of the carbon analogues despite some quantitative discrepancies. One example is the singlet silylene (SiH_2). The first theoretical study for its reactions with s-bonded systems HX can be dated to as early as 1984.[27d] Several studies have focused on the insertion reaction producing H_3SiX[10,27] similar to those for the singlet CH_2. Only from 2001 have the other reactions such as H_2-elimination leading to HSiX + H_2 come into consideration. For the simplest monovalent Si-radical, SiH, only the insertion reaction has been studied.[12,13]

Recently, we have been interested in the silicon-containing cation, $[Si,C,N]^+$, which contains all heavy atoms. It can be produced during the chemical vaporization decomposition (CVD) processes of SiCN films and can further react with minute gaseous molecules such as hydrocarbons. The $[Si,C,N]^+$ ion might also be related to the astrophysical chemistry. Recently, the silicon chemistry in space has received increasing attention. It has been shown that the depletion of silicon in space is just slighter less than those of C, N, and O.[29] It is believed that with more spectroscopic data available, more silicon-bearing species could be detected. Recently, the first nonhydrogenated ternary silicon-bearing radicals SiCN and SiNC have been detected in space.[30] More complex molecules such as [H,Si,C,N] (with HSiCN, HSiNC, and HCNSi isomers)[31] and $[H_3,Si,C,N]$ (with H_3CNSi, H_3SiCN, and H_3SiNC isomers)[32] have also been characterized in laboratory. Upon electron impact-induced ionization or radiation, these SiCN-containing species could generate $[Si,C,N]^+$. The reactions of the $[Si,C,N]^+$ ion with stable molecules then can form new silicon-bonded species. The analogous C_2N^+ ion has been extensively studied,[33−38] for which the carbene insertion is the major pathway when it reacts with σ-bonded systems. To the best of our knowledge, only the structures and energetics of $SiCN^+$ and its isomeric form $SiNC^+$ have been previously studied.[39]

Recently, we initiated a preliminary theoretical study on the $SiCN^+/SiNC^+ + H_2O$ reactions.[40] The results indicated that the 1,2-H-shift (associated with "silylene insertion") is of little importance. Instead, the reactions most feasibly undergo the 1,4-H-shift followed by the final dissociation to $HOSi^+$ + HCN (major) and $HOSi^+$ + HNC (minor). Moreover, the −NC↔−CN conversion is very easy. In the present paper, we extend the study of the ion−molecule reactions of $SiCN^+/SiNC^+$ with a series of σ-bonded molecules H_2, CH_4, HF, and NH_3, which are important gaseous species in CVD environments and have all been detected in space. Particularly, NH_3 and HF both possess

* Author to whom correspondence should be addressed. E-mail: yhdd@mail.jlu.edu.cn; fax: +86-431-8498889.

10.1021/jp050876y CCC: $30.25
Published on Web 06/01/2005

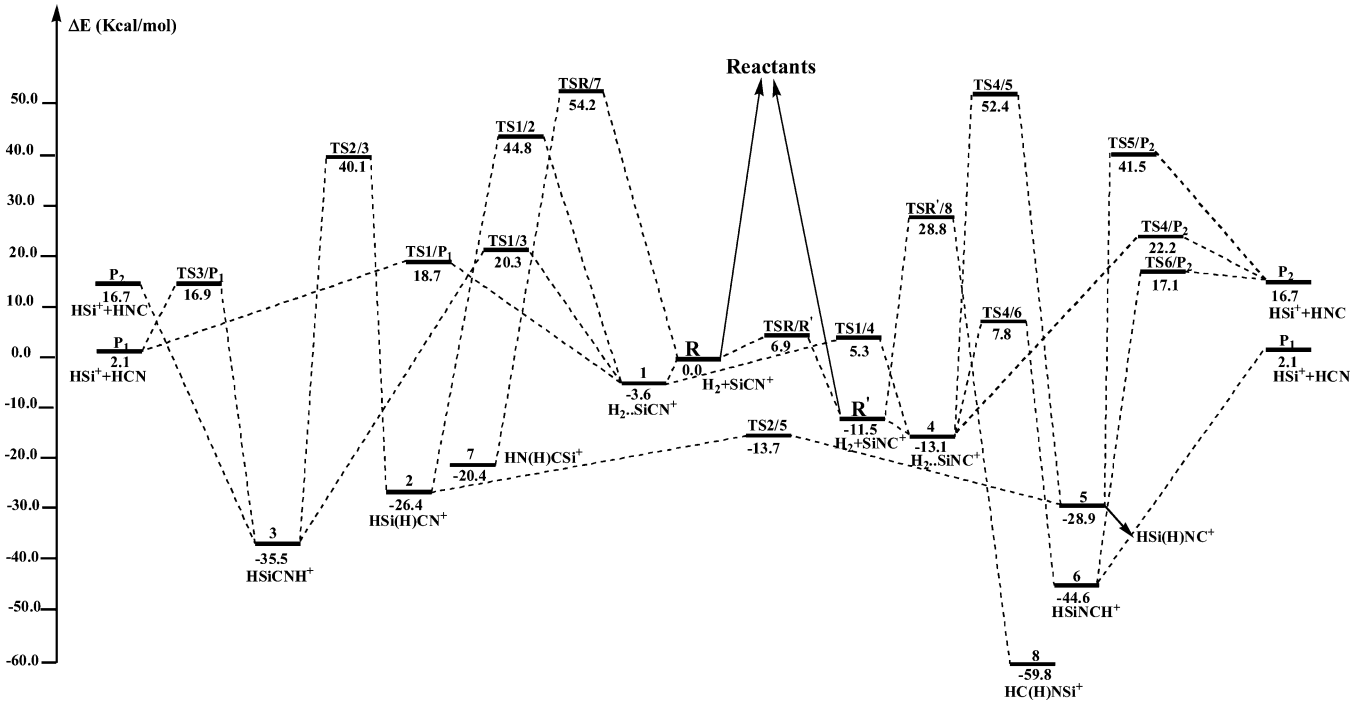

Figure 1. Schematic pathways for the $SiCN^+/SiNC^+ + H_2$ reaction. Relative energies are calculated at the CCSD(T)/6-311+G(2df,p)//B3LYP/6-311G(d,p)+ZPVE level.

lone pairs as H_2O does, whereas H_2 and CH_4 are archetypes of lone pair deficient molecules. We want to know (1) whether the title reactions have the insertion as their major pathway similar to those of neutral monovalent SiH radical, atomic Si^+, and analogous C_2N^+ ion and (2) what kind of silicon-bonded species the reactions can lead to. By means of a detailed search for possible reaction pathways, a distinct mechanism other than that for the reactions of atomic Si^+ and neutral SiH is revealed in the present paper.

2. Theoretical Methods

All calculations are carried out using Gaussian 03 program packages.[41] The geometries of all the reactants, products, intermediates, and transition states are optimized using hybrid density functional B3LYP method with the 6-311G(d,p) basis set. Frequency calculations are performed at the same level to check whether the obtained stationary point is an isomer or a first-order transition state. To confirm that the transition state connects designated intermediates, we also perform intrinsic reaction coordinate (IRC) calculations at the B3LYP/6-311G-(d,p) level. In addition, the energies of all species are refined at the CCSD(T)/6-311+G(2df,p) level using the B3LYP/6-311G-(d,p)-optimized geometries. These are denoted as single-point CCSD(T)/6-311+G(2df,p)//B3LYP6-311G(d,p) energies. The B3LYP/6-311G(d,p) zero-point vibrational energies (ZPVE) are also included. Finally, to test the reliability, the more composite Gaussian-3//B3LYP/6-31G(d) method (based on a series of single-point energy calculations) is preformed on some critical structures for the $SiCN^+/SiNC^+ + HF$ reactions.

3. Results and Discussions

The results of the $SiCN^+/SiNC^+ + H_2O$ reactions[40] are also included for systematic discussion. For the five model ion−molecule reactions $SiCN^+/SiNC^+ + HX$ (X = H, CH_3, F, OH, NH_2), the schematic possible reaction pathways are depicted in Figures 1−5, respectively. The barriers of the relevant pathways are shown in Table 1. For each reaction, the energy of the reactant $SiCN^+ + HX$ is set to zero for reference. Unless otherwise specified, the energies are referred to as CCSD(T)/6-311+G(2df,p)//B3LYP/6-311G(d,p)+ZPVE (simplified as CCSD(T)//B3LYP) values. The symbol **TSm/n** is used to denote the transition state connecting the isomers **m** and **n**. Moreover, to test the reliability of the CCSD(T)//B3LYP results, we performed Gaussian-3//B3LYP/6-31G(d) calculations (simplified as G3//B3LYP) for critical structures of the $SiCN^+/SiNC^+ +$ HF reactions. For simplicity, only the main features of the reactions are presented in the context. The other information is collected in supporting materials.

3.1 Association. The $[Si,C,N]^+$ ion has two isomeric forms $SiNC^+$ and $SiCN^+$ with the latter 11.5 kcal/mol higher. On one hand, the nucleophilic attack should a priori take place at the terminal Si-atom with the localized positive charge (i.e., 1.16e for $SiNC^+$ and 1.12e for $SiCN^+$). On the other hand (see Scheme 1), the Si-atom of the $[Si,C,N]^+$ ion has one electron lone pair orbital (HOMO) and two degenerate π-bonded vacant orbitals (LUMO) and can easily interact with the electron donors such as NH_3, H_2O, and HF. Consequently, the long-range electrostatic and donor−acceptor interaction can barrierlessly lead to the ion−molecule adduct HX...SiY^+ (Y = −CN and −NC). The thermodynamic stability of HX...SiY^+ relative to the reactant $SiY^+ + HX$ is −58.9, −45.4, −19.2, −15.6, and −3.6 kcal/mol for Y = −CN and −51.4, −39.0, −16.1, −10.3, and −1.6 kcal/mol for Y = −NC, respectively. The stability of the adduct decreases in the order of X = NH_2 > OH > F > CH_3 > H, which is consistent with the decreased electron-donating ability of X. Surely, reaction with the strongest electron donor NH_3 results in the greatest stabilization for the adduct, whereas that with H2 has negligible stabilization because of the absence of lone pair and charge center. The relative stability of HX...SiY^+ for Y = −CN is higher than that for Y = −NC, which can be interpreted by the respective LUMO energies −0.40245 and −0.37952 au (the lower value means the higher ability to accept electrons).

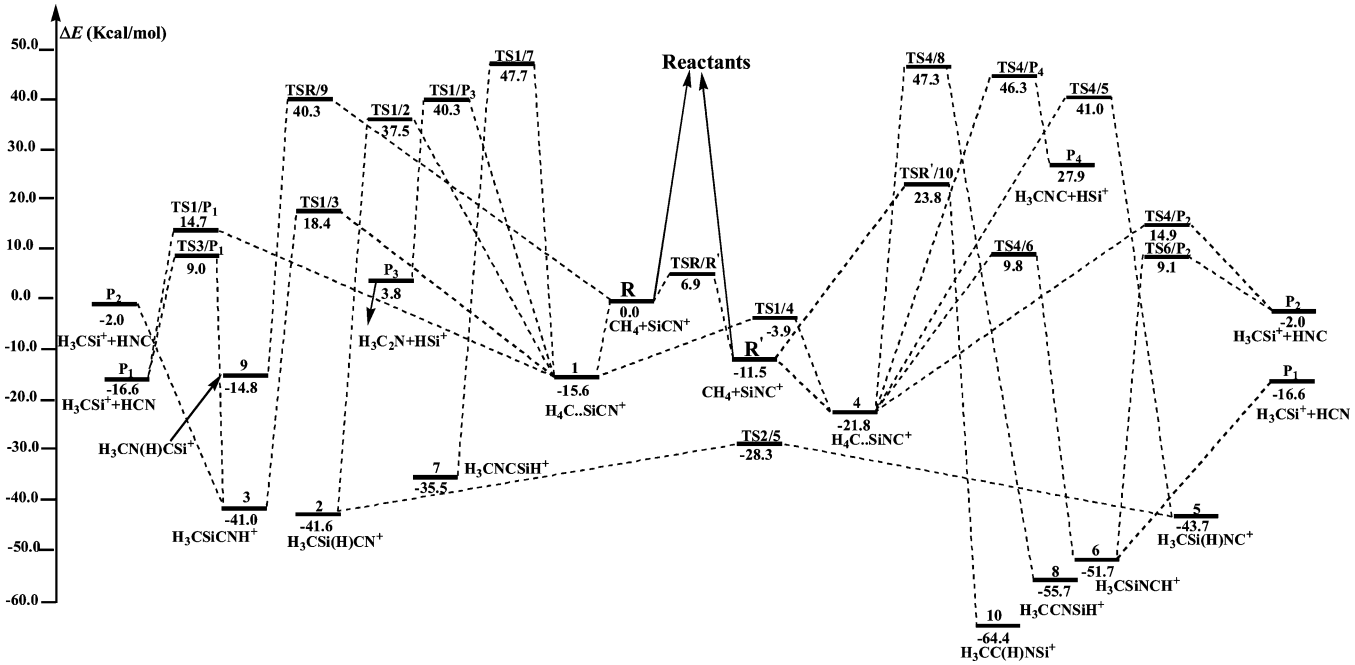

Figure 2. Schematic pathways for the $SiCN^+/SiNC^+ + CH_4$ reaction. Relative energies are calculated at the CCSD(T)/6-311+G(2df,p)//B3LYP/6-311G(d,p)+ZPVE level.

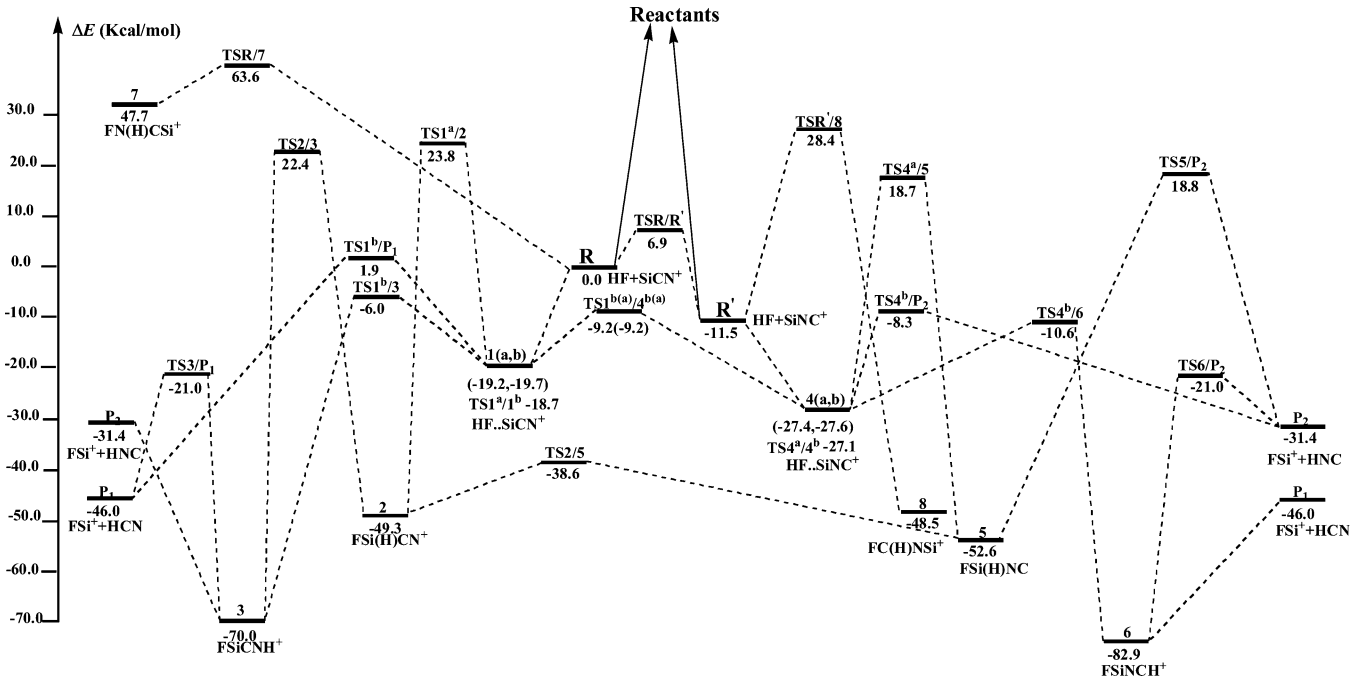

Figure 3. Schematic pathways for the $SiCN^+/SiNC^+ + HF$ reaction. Relative energies are calculated at the CCSD(T)/6-311+G(2df,p)//B3LYP/6-311G(d,p)+ZPVE level.

3.2 Isomerization, Dissociation, and Reaction Mechanism. Let us discuss further evolution of the initially formed ion−molecule adduct $HX...SiY^+$ (Y = −CN and −NC). On the basis of the schematic pathways of the five model reactions in Figures 1−5, we can deduce that generally there are four kinds of processes, namely, −CN↔−NC conversion, 1,4-H-shift (forming $XSiYH^+$), 1,3-H-shift (forming $SiX^+ + HY$), and 1,2-H-shift (forming $XSiHY^+$). The −CN→−NC conversion barriers are of the averaged value 12 kcal/mol, while the −NC→−CN values are almost constant as 18 kcal/mol (see Table 1). Generally, for the $HX...SiY^+$ adduct, the −CN→−NC interconversion is the most feasible of the four processes. The exception is $HF...SiNC^+$, for which the −NC→−CN barrier (18.4 kcal/mol) is slightly higher than the corresponding 1,4-H-shift barrier (17.0 kcal/mol). For the analogous $C_2N^+ + H_2O$ reaction,[37] the respective −CN→−NC and −NC→−CN barriers are very large as 46.7 and 45.2 kcal/mol. The sharp discrepancy can be ascribed to the fact that the $HXCY^+$ adduct has CY double-bonding character, whereas the $HX...SiY^+$ adduct has no or very weak such character. This is understandable because silicon is reluctant to form multiple bonding while carbon prefers to form multiple bonding.

The 1,4-H-shift step is generally more competitive than the 1,3-H-shift step with two exceptions $SiCN^+ + H_2$ and $SiCN^+ + CH_4$. Noticeably, (i) the 1,2-H-shift process, which is

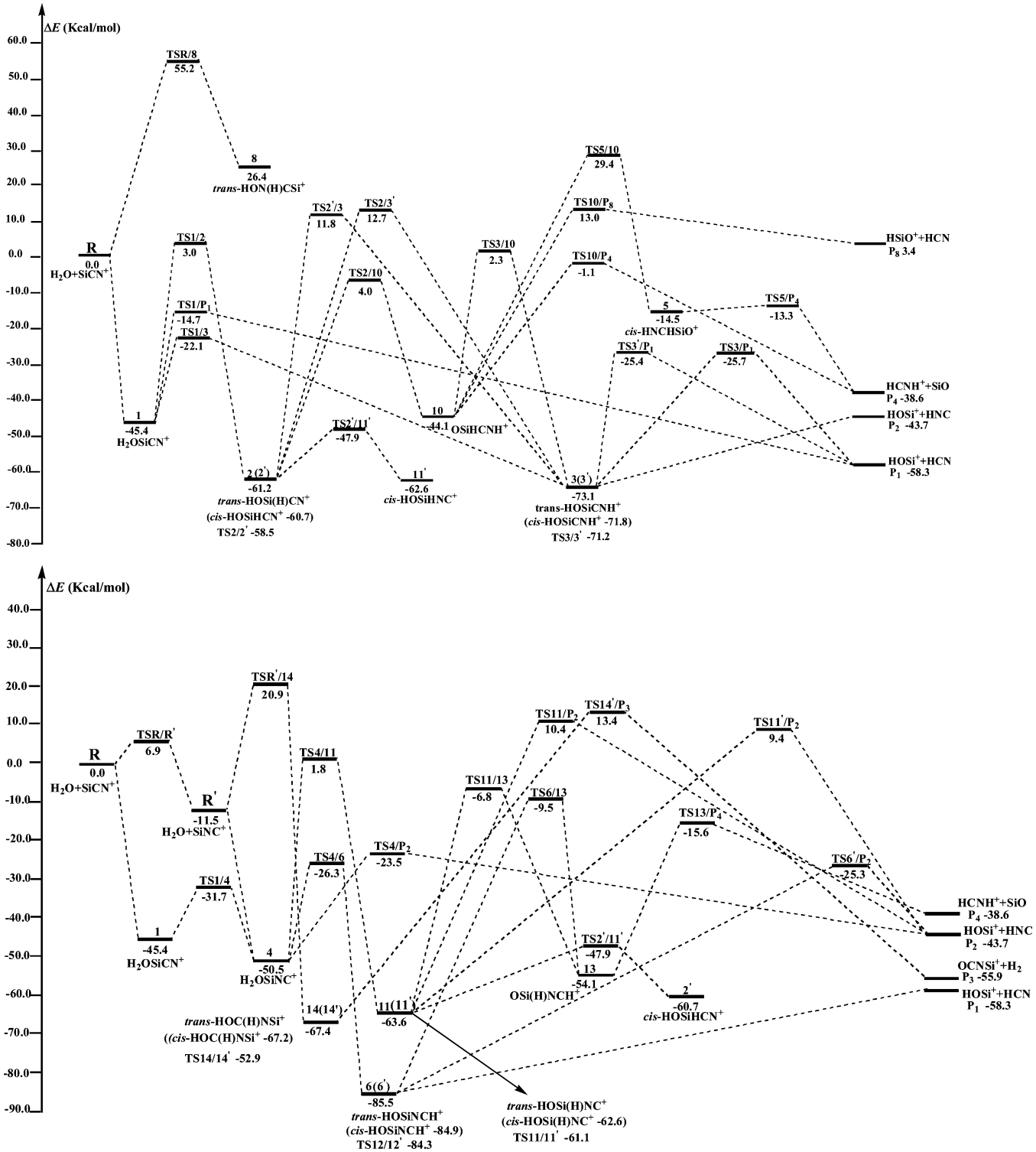

Figure 4. (a) Schematic pathways for the $SiCN^+ + H_2O$ reaction. Relative energies are calculated at the CCSD(T)/6-311+G(2df,p)//B3LYP/6-311G(d,p)+ZPVE level. (b) Schematic pathways for the $SiNC^+ + H_2O$ reaction. Relative energies are calculated at the CCSD(T)/6-311+G(2df,p)//B3LYP/6-311G(d,p)+ZPVE level.

associated with the "silylene insertion", has the highest barrier of all the considered species and (ii) the 1,2-H-shift barrier for Y = −NC is somewhat higher than that for Y = −CN. Both points can be explained by the adiabatic singlet−triplet energy gaps (ΔE_{S-T}), which is considered here as a rough criterion for the insertion ability when one of the lone pair electrons is promoted to the vacant orbital. The ΔE_{S-T} values for $SiCN^+$ and $SiNC^+$ are rather large as 68.07 and 70.71 kcal/mol, respectively, at the B3LYP/6-311G(d) level. Such a large energy gap makes the H-atom shifted to the faraway atoms (1,4- or 1,3-H-shift) rather than to the neighboring atom (1,2-H-shift) (for point i). Also, the larger ΔE_{S-T} value means the lower insertion stability (for point ii). The unfavorable silylene insertion for the $SiY^+ + HX$ reactions contrasts sharply to the $C_2N^+ + H_2O/H_2S$ reactions for which the carbene insertion is the major pathway.[37,38] The respective B3LYP/6-311G(d) DES-T values for CCN^+ and CNC^+ are as low as 30.20 and 42.00 kcal/mol.

For all the considered reactions, the 1,4-H-shift step is the most feasible for HX...$SiNC^+$ **4**, irrespective of the cyano

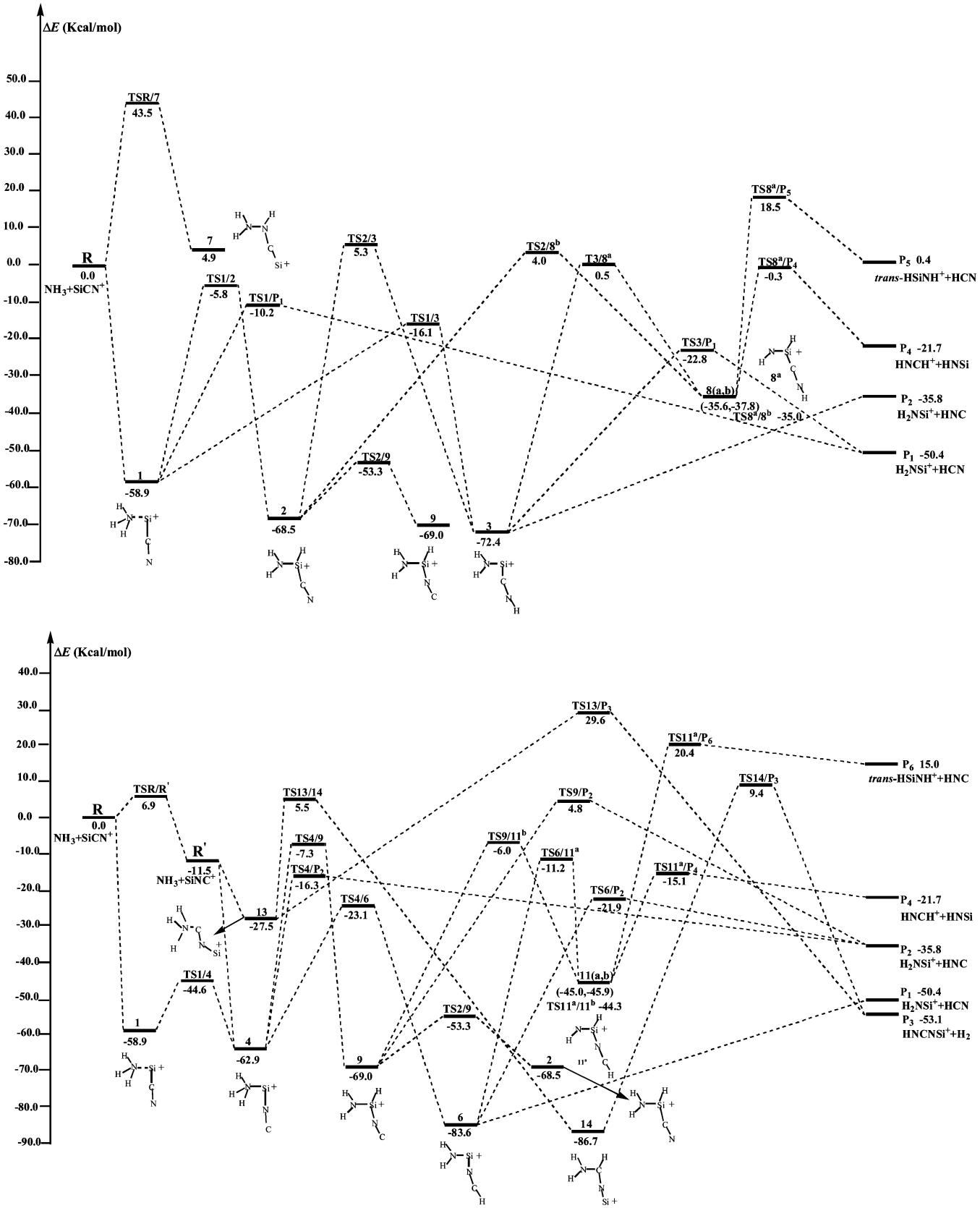

Figure 5. (a) Schematic pathways for the $SiCN^+ + NH_3$ reaction. Relative energies are calculated at the CCSD(T)/6-311+G(2df,p)//B3LYP/6-311G(d,p)+ZPVE level. (b) Schematic pathways for the $SiNC^+ + NH_3$ reaction. Relative energies are calculated at the CCSD(T)/6-311+G(2df,p)//B3LYP/6-311G(d,p)+ZPVE level.

exchange. The corresponding transition state **TS4/6** is energetically lower than all the transition states for HX...$SiCN^+$ **1**. Thus, the dominant reaction scheme for **R** $SiCN^+ + HX$ follows that of **R′** $SiNC^+ + HX$ via the easy −CN→−NC conversion. Starting from **R** and **R′**, the respective most feasible pathways toward fragmentation can be written as

Path **R**(X): $SiCN^+ + HX \rightarrow$ HX...$SiCN^+$ **1**→HX...$SiNC^+$ **4**→$XSiNCH^+$ **6**→$\mathbf{P_1}$ $SiX^+ + HCN$

TABLE 1: The Barriers (in kcal/mol) for the −CN↔−NC Conversion, 1,4-Shift, 1,3-H-Shift, and 1,2-H-Shift Processes of the Adduct HX...SiY$^+$ [a]

	Y = −CN					Y* = −NC				
	X = H	X = CH_3	X = F	X = OH	X = NH_2	X = H	X = CH_3	X = F	X = OH	X = NH_2
−CN↔−NC	8.9	11.7	10.5	13.7	14.3	18.4	17.9	18.4	18.8	18.3
			10.9					*18.4*		
1,4-H-shift	23.9	34.0	13.7	23.3	42.8	20.9	31.6	17.0	24.2	39.8
			13.2					*16.2*		
1,3-H-shift	22.3	30.3	21.6	30.7	48.7	35.3	36.7	19.3	27.0	46.6
			20.9					*18.5*		
1,2-H-shift	58.4	53.1	43.5	48.4	53.1	65.5	62.8	46.3	48.7	55.6
			42.4					*45.3*		

[a] Relative energies are calculated at the CCSD(T)/6-311+G(2df,p)//B3LYP/ 6-311G(d,p)+ZPVE and Gaussian-3//B3LYP/6-31G(d) (in italics) levels.

SCHEME 1: Nucleophilic Attack and Silylene Insertion Process

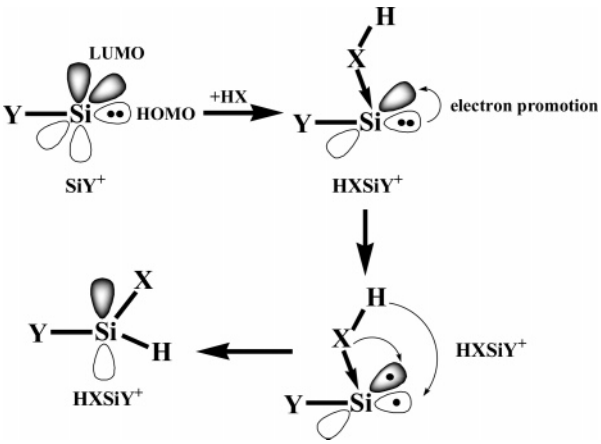

Path **R′**(X): $SiNC^+ + HX \rightarrow HX...SiNC^+$ **4**$\rightarrow XSiNCH^+$ **6**$\rightarrow$**P$_1$** $SiX^+ + HCN$.

Both reactants most feasibly lead to the same product **P$_1$** $SiX^+ + HCN$ in major amounts.

The second lowest-energy transition state for $HX...SiNC^+$ **4** is **TS4/P$_2$** (1,3-H-shift) which is associated with product **P$_2$** $SiX^+ + HNC$. However, competition of the 1,4- or 1,3-H-shift processes of $HX...SiCN^+$ **1** must be considered. For $HX...SiCN^+$ **1**, the lowest-energy transition state for X = F, OH, and NH_2 is 1,4-H-shift **TS1/3** (at −6.0, −22.1, and −16.1 kcal/mol, respectively) leading to **P$_2$** $SiX^+ + HNC$ via $HXSiCNH^+$ **3**, while that for X = H and CH_3 is 1,3-H-shift **TS1/P$_1$** (at 18.7 and 14.7 kcal/mol, respectively) leading to **P$_1$** $SiX^+ + HCN$. These transition states are energetically very close to **TS4/P$_2$** (at −8.3, −23.5, −16.3, 22.2, and 14.9 kcal/mol for X = F, OH, NH_2, H, and CH_3, respectively). For X = H, the 1,4-H-shift **TS1/3** (at 20.3 kcal/mol) leading to **P$_1$** $SiX^+ + HCN$ or **P$_2$** $SiX^+ + HNC$ should also be included. Altogether, the second most feasible product for both reactions is either **P$_2$** $SiX^+ + HNC$ or **P$_2$** $SiX^+ + HNC$ plus **P$_1$** $SiX^+ + HCN$ in minor amounts.

As a result, the overall reactions can be expressed as $SiCN^+/SiNC^+ + HX \rightarrow SiX^+ + HCN(major)/HNC(minor)$, pointing to a group exchange (X and −CN or −NC) between the reactants. Thus, the reactions formally correspond to the "nucleophilic substitution" mechanism. Specifically, the reactions of $SiCN^+/SiNC^+$ with strong electron donors NH_3, H_2O, and HF can easily take place even at low temperatures because the involved intermediates and transition states of the relevant pathways forming the major and minor products are all lower in energy than the reactants (for $SiNC^+$ + HF reaction, the lowest **TS4/6** is just 0.9 kcal/mol above the reactant) (see Figures 3−5). However, the situation for the reactions of $SiCN^+/SiNC^+$ with completely saturated CH_4 and H_2 is quite different. The $SiNC^+ + CH_4/H_2 \rightarrow SiCH_3^+/SiH^+ + HCN$ reactions have to overcome very large barriers of 21.3/19.3 kcal/mol (via **TS4/6**) and are unlikely to take place. Yet the $SiCN^+ + CH_4/H_2 \rightarrow SiCH_3^+/SiH^+ + HCN$ reactions can proceed at high temperatures with much smaller barriers 9.8/7.8 kcal/mol (via **TS4/6**). At low temperatures, there exists a route for the barrierless $SiCN^+ \rightarrow SiNC^+$ conversion: $SiCN^+ + CH_4 \rightarrow HCH_3...SiCN^+ \rightarrow HCH_3...SiNC^+ \rightarrow SiNC^+ + CH_4$, in which CH_4 acts as a gaseous organic catalyst.

Let us make comparative discussions between various computational levels (see Supporting Information). First, for the presently studied $SiCN^+/SiNC^+ + HX$ (X = H, CH_3, F, NH_2) reactions which contain a total of 152 species (reactants, isomers, and transition states), the agreement between the B3LYP/6-311G(d,p) and CCSD(T)/6-311+G(2df,p) results is reasonable with the averaged absolute difference 2.37 kcal/mol. The −CN↔−NC conversion and nitrene and carbene-insertion processes usually have large differences. In particular, the nitrene-insertion **TSR/7**, isomer $FN(H)CSi^+$ **7**, and carbene-insertion **TSR′/8** for the $SiCN^+/SiNC^+ + HF$ reaction have the largest differences as 9.9, 10.0, and 11.7 kcal/mol, respectively. Fortunately, the two processes are not important for the reactions of $SiCN^+/SiNC^+$. Second, we are concerned with the influence of the zero-point vibrational energies (ZPVE) on the relative energies. The averaged absolute ΔZPVE values for the 152 species are 1.81 kcal/mol. The large values 8.4, 7.7, and 9.4 kcal/mol are associated with the nitrene-insertion isomer $HN(H)CSi^+$ **7**, carbene-insertion isomer $HC(H)NSi^+$ **8**, and donor−acceptor adduct H_3NCNSi^+ **13**, respectively. In addition, the relative stability of the transition states for the reactions of $SiCN^+/SiNC^+$ with NH_3, HF, and CH_4 is generally increased upon ZPVE inclusion, whereas that for the reactions of $SiCN^+/SiNC^+$ with H_2 is decreased. Also, the relative stability of the intermediate isomers for the reactions of $SiCN^+/SiNC^+$ with NH_3, HF, and H_2 is generally decreased. The ZPVE correction even reverses the energy order of the products **P$_1$** $H_2NSi^+ + HCN$ and **P$_3$** $HNCNSi^+ + H_2$ for the $SiCN^+/SiNC^+ + NH_3$ reaction. At the CCSD(T)/6-311+G(2df,p)//B3LYP/6-311G(d,p) level, **P$_3$** (−48.1) lies slightly above **P$_1$** (−50.1). Yet after ZPVE correction, **P$_3$** (−53.1) lies slightly below **P$_1$** (−50.4).

Third, the more composite G3//B3LYP calculations are carried out on some critical structures for the model reaction $SiCN^+/SiNC^+ + HF$ to test the reliability of the CCSD(T)//B3LYP results. For the 14 species **1^a** (−19.2, *−18.7*), **1^b** (−19.7, *−19.2*), **4^a** (−27.4, *−26.5*), **4^b** (−27.6, *−26.7*), **TS1^a/1^b** (−18.7, *−17.9*), **TS1^a/2** (23.8, *23.7*), **TS1^a/4^a** (−9.2, *−8.4*), **TS1^b/P$_1$** (1.9, *1.7*), **TS1^b/3** (−6.0, *−6.0*), **TS1^b/4^b** (−9.2, *−8.3*), **TS4^a/4^b** (−27.1, *−26.0*), **TS4^a/5** (18.7, *18.8*), **TS4^b/P$_2$** (−8.3, *−8.2*), and **TS4^b/6** (−10.6, *−10.5*), we can find that the relative

energies at the G3//B3LYP level (in italics) are in excellent agreement with those at the CCSD(T)//B3LYP level. Consequently, as listed in Table 1, the G3//B3LYP barriers (*10.9*, *13.2*, *20.9*, and *42.4* kcal/mol via **TS1^b/4^b**, **TS1^b/3**, **TS1^b/P$_1$**, and **TS1^a/2**, respectively) for the −CN↔−NC, 1,4-shift, 1,3-H-shift, and 1,2-H-shift processes of the adduct HF...$SiCN^+$ are very close to the corresponding CCSD(T)//B3LYP values (10.5, 13.7, 21.6, and 43.5 kcal/mol). Similarly, for the HF...$SiNC^+$ adduct, the G3//B3LYP barriers (*18.4*, *16.2*, *18.5*, and *45.3* kcal/mol via **TS1^b/4^b**, **TS4^b/6**, **TS4^b/P$_2$**, and **TS4^a/5**, respectively) for the three processes are also very close to the corresponding CCSD(T)//B3LYP values (18.4, 17.0, 19.3, and 46.3 kcal/mol). Moreover, for the $SiCN^+/SiNC^+ + H_2O$ reactions, it was found that both the structural parameters and relative energies at the CCSD(T)//B3LYP level are generally in good agreement with those at the CCSD(T)//MP2 level.[40] Therefore, the present CCSD(T)//B3LYP results for the $SiCN^+/SiNC^+ + HX$ reactions are expected to provide reliable prediction for future experimental investigations.

3.3 Laboratory and Astrophysical Implications. One worthwhile result reported here is that the ion−molecule reactions of $SiCN^+/SiNC^+$ have nucleophilic substitution rather than silylene insertion as their major pathway. Although silicon differs greatly from carbon in the s,p-hybridization ability, it has been usually considered that monovalent or divalent silicon species will still show insertion behavior toward σ-bonded species as carbon species behave. In fact, not until recently[23−26] have the other pathways of SiH_2 with σ-bonded species other than insertion been taken into consideration. This may partially explain the limited theoretical investigations for the reactions of silicon-containing ions. However, the present results for the reactions of $SiCN^+/SiNC^+$ with five model HX molecules clearly show that the significantly decreased insertion ability even changes the reaction mechanism. The present computational study may be the first systematic study for the reactions of the Si-bearing ions that comprise three heavy atoms.

In addition to the importance for mechanistic study, the model ion−molecule reactions have potential applications in the chemical vaporization decomposition or astrophysical chemistry. On one hand, these σ-bonded species are important environmental or minute gases. Under combustion condition, the $SiCN^+/SiNC^+$ ions can be effectively destructed by HX (especially those with an electron lone pair) forming new Si−X bonded ions. Moreover, the reactions can dominantly generate HCN, which is an important reagent in the film preparation. On the other hand, the fact that the $SiCN^+/SiNC^+ + HX$ (X = NH_2, OH, and F) reactions have no or minute barriers makes these ion−molecule processes very promising in space, where the environmental temperature is usually very low (10−100 K). These reactions can effectively produce new ionized species with Si−N, Si−O, and Si−F bonds.

4. Conclusions

Detailed theoretical investigations have been performed for the reactions of $SiCN^+/SiNC^+$ with five σ-bonded molecules H_2, CH_4, HF, H_2O, and NH_3 for the purpose of unraveling the ion−molecule mechanism of the $[Si,C,N]^+$ ion that contains all heavy atoms. The results can be summarized as follows:

(1) Initially, both the $SiCN^+/SiNC^+ + HX$ reactions can take the effective nucleophilic attack (except for X = H) at the positive Si-site via the donor−acceptor interaction, forming the ion−molecule adducts HX...$SiCN^+$/HX...$SiNC^+$. Subsequently, the adducts can lead to the products **P$_1$** $SiX^+ + HCN$ (major) and **P$_2$** $SiX^+ + HNC$ (minor) via the 1,4- or 1,3-H-shift. The overall $SiCN^+/SiNC^+ + HX$ reactions have "nucleophilic substitution" as their major pathway.

(2) The silylene insertion cannot compete with the 1,4- and 1,3-H-shift steps. The significantly lowered insertion ability of $SiCN^+/SiNC^+$ as compared to the analogous CCN^+/CNC^+ can be explained by the fact that the former ions have much larger singlet−triplet energy gaps than the latter.

The calculated results presented here are useful for gaining insight into the reactive $[Si,C,N]^+$ chemistry which could be related to the combustion and interstellar processes. Future laboratory investigations on the $[Si,C,N]^+$ chemistry are strongly desirable.

Acknowledgment. This work is supported by the National Natural Science Foundation of China (No. 20103003), Doctor Foundation of Educational Ministry, and Excellent Young Teacher Foundation of Ministry of Education of China.

Supporting Information Available: Computational details for the reactions $SiCN^+/SiNC^+ + HX$ (X = H, CH_3, NH_2, F). This material is available free of charge via the Internet at http://pubs.acs.org.

References and Notes

(1) Wlodek, S.; Fox, A.; Bohme, D. K. *J. Am. Chem. Soc.* **1991**, *113*, 4461.
(2) Glosík, J.; Zakouøil, P.; Lindinger, W. *J. Chem. Phys.* **1995**, *103*, 6490.
(3) Glosík, J.; Zakouøil, P.; Lindinger, W. *Int. J. Mass Spectrom. Ion Processes* **1995**, *149/150*, 499.
(4) Glosík, J.; Zakouøil, P.; Lindinger, W. *Int. J. Mass Spectrom. Ion Processes* **1995**, *145*, 155.
(5) Ferguson, E. E.; Fahey, D. W.; Fehsenfeld, F. C.; Albritton, D. L. *Planet. Space Sci.* **1981**, *19*, 307.
(6) Glosík, J.; Zakouøil, P. *J. Chem. Phys.* **1995**, *103*, 6490.
(7) Chaabane, N.; Vach, H.; Cabarrocas, P. R. i. *J. Phys. Chem. A* **2004**, *108*, 1818.
(8) Glosík, J.; Zakouøil, P.; Luca, A. *Int. J. Mass Spectrom.* **2003**, *223−224*, 539.
(9) Haller, I. *J. Phys. Chem.* **1990**, *94*, 4135.
(10) Abernathy, R. N.; Lampe, F. W. *Int. J. Mass Spectrom. Ion Processes* **1983**, *51*, 3.
(11) Gordon, M. S.; Gano, D. R. *J. Am. Chem. Soc.* **1984**, *106*, 5421.
(12) Wang, Z.-X.; Huang, M.-B. *J. Chem. Soc., Faraday Trans.* **1998**, *94* (5), 635 and references therein.
(13) Wang, Z.-X.; Huang, M.-B. *J. Phys. Chem. A.* **1998**, *102*, 229 and references therein.
(14) Jasinski, J. M.; Becerra, R.; Walsh, R. *Chem. Rev.* **1995**, *95*, 1203.
(15) Becerra, R.; Frey, H. M.; Mason, B. P.; Walsh, R. *Chem. Phys. Lett.* **1991**, *185*, 415.
(16) Al-Rubaiey, N.; Wahsh, R. *J. Phys. Chem.* **1994**, *98*, 5303.
(17) Becerra, R.; Cannady, J. P.; Walsh, R. *J. Phys. Chem. A* **1999**, *103*, 4457.
(18) Becerra, R.; Carpenter, I. W.; Gutsche, G. J.; King, K. D.; Lawrance, W. D.; Staker, W. S.; Walsh, R. *Chem. Phys. Lett.* **2001**, *333*, 83.
(19) Becerra, R.; Cannady, J. P.; Walsh, R. *J. Phys. Chem. A* **2001**, *105*, 1897.
(20) Becerra, R.; Cannady, J. P.; Walsh, R. *J. Phys. Chem. A* **2002**, *106*, 4922.
(21) Becerra, R.; Cannady, J. P.; Walsh, R. *J. Phys. Chem. A* **2002**, *106*, 11558.
(22) Takeuchi, N.; Kanai, Y.; Selloni, A. *J. Am. Chem. Soc.* **2004**, *126*, 15890.
(23) Alexander, U. N.; King, K. D.; Lawrance, W. D. *J. Phys. Chem. A* **2002**, *106*, 973.
(24) Heaven, M. W.; Metha, G. F.; Buntine, M. A. *J. Phys. Chem. A* **2001**, *105*, 1185.
(25) Becerra, R.; Cannady, J. P.; Walsh, R. *J. Phys. Chem. A* **2003**, *107*, 11049.
(26) Becerra, R.; Goldberg, N.; Cannady, J. P.; Almond, M.; Ogden, J. S.; Walsh, R. *J. Am. Chem. Soc.* **2004**, *126*, 6816.
(27) (a) Gano. D. R.; Gordon, M. S.; Boatz, J. A. *J. Am. Chem. Soc.* **1991**, *113*, 6711. (b) Sosa, C.; Schlegel, H. B. *J. Am. Chem. Soc.* **1984**, *106*, 5847. (c) Sakai, S.; Nakamura, M. *J. Phys. Chem.* **1993**, *97*, 4960. (d) Raghavachari, K.; Chandrasekhar, J.; Gordon, M. S.; Dykema, K. J. *J. Am. Chem. Soc.* **1984**, *106*, 5853.

(28) (a) Tachibana, A.; Kawauchi, S.; Yoshida, N.; Yamabe, T.; Fukui, K. *J. Mol. Struct*. **1993**, *300*, 501. (b) Redondo, P.; Sagüillo, A.; Barrientos, C.; Largo, A. *J. Phys. Chem. A* **1999**, *103*, 3310. (c) Largo, A.; Barrientos, C. *J. Phys. Chem*. **1994**, *98*, 3978 (d) Flores, J. R. *J. Phys. Chem*. **1992**, *96*, 4414. (e) Flores, J. R.; Redondo, P.; Azpeleta, S. *Chem. Phys. Lett*. **1995**, *240*, 193. (f) Srinivas, R.; Hrušák, J.; Sülzle, D.; Böhme, D. K.; Schwarz, H. *J. Am Chem. Soc*. **1992**, *114*, 2802.

(29) McCarthy, M. C.; Gottlieb, C. A.; Thaddeus, P. *Mol. Phys*. **2003**, *101*, 697.

(30) Guelin, M.; Muller, S.; Cernicharo, J.; Apponi, A. J.; McCarthy, M. C.; Gottlieb, C. A.; Thaddeus, P. *Astron. Astrophys*. **2000**, *363*, L9.

(31) Sanz, M. E.; McCarthy, M. C.; Thaddeus, P. *Astrophys. J*. **2002**, *577*, L71.

(32) Maier, G.; Reisenauer, H. P.; Egenolf, H.; Glatthaar, J. *Eur. J. Org. Chem*. **1998**, 1307.

(33) Bohme, D. K.; Wlidek, S.; Raksit, A. B.; Schiff, H. I.; Mackay, G. I.; Keskinen, K. J. *Int. J. Mass Spectrom. Ion Processes* **1987**, *81*, 123.

(34) McEwan, M. J.; Anicich, V. G.; Huntress, W. T. *Int. J. Mass Spectrom. Ion Phys*. **1983**, *50*, 179.

(35) Haese, N. N.; Woods, R. C. *Astrophys. J*. **1981**, **246**, L51.

(36) Yoshimine, M.; Kraemer, W. P. *Chem. Phys. Lett*. **1982**, *90*, 145.

(37) Tao, Y. G.; Ding, Y. H.; Liu, J. J.; Li, Z. S.; Huang, X. R.; Sun, C. C. *J. Chem. Phys.* **2001**, *116*, 5.

(38) Tao, Y. G.; Ding, Y. H.; Liu, J. J.; Li, Z. S.; Huang, X. R.; Sun, C. C. *J. Phys. Chem. A* **2002**, *106*, 2949.

(39) Largo-Cabrerizo, A.; Barrientos, C. *Chem. Phys. Lett*. **1988**, *148*, 79.

(40) Wang, J.; Ding, Y. H.; Sun, C. C. *J. Chem. Phys*. **2005**, *122*, 4309.

(41) Frisch, M. J.; Trucks, G. W.; Schlegel, H. B.; Scuseria, G. E.; Robb, M. A.; Cheeseman, J. R.; Montgomery, J. A., Jr.; Vreven, T.; Kudin, K. N.; Burant, J. C.; Millam, J. M.; Iyengar, S. S.; Tomasi, J.; Barone, V.; Mennucci, B.; Cossi, M.; Scalmani, G.; Rega, N.; Petersson, G. A.; Nakatsuji, H.; Hada, M.; Ehara, M.; Toyota, K.; Fukuda, R.; Hasegawa, J.; Ishida, M.; Nakajima, T.; Honda, Y.; Kitao, O.; Nakai, H.; Klene, M.; Li, X.; Knox, J. E.; Hratchian, H. P.; Cross, J. B.; Bakken, V.; Adamo, C.; Jaramillo, J.; Gomperts, R.; Stratmann, R. E.; Yazyev, O.; Austin, A. J.; Cammi, R.; Pomelli, C.; Ochterski, J. W.; Ayala, P. Y.; Morokuma, K.; Voth, G. A.; Salvador, P.; Dannenberg, J. J.; Zakrzewski, V. G.; Dapprich, S.; Daniels, A. D.; Strain, M. C.; Farkas, O.; Malick, D. K.; Rabuck, A. D.; Raghavachari, K.; Foresman, J. B.; Ortiz, J. V.; Cui, Q.; Baboul, A. G.; Clifford, S.; Cioslowski, J.; Stefanov, B. B.; Liu, G.; Liashenko, A.; Piskorz, P.; Komaromi, I.; Martin, R. L.; Fox, D. J.; Keith, T.; Al-Laham, M. A.; Peng, C. Y.; Nanayakkara, A.; Challacombe, M.; Gill, P. M. W.; Johnson, B.; Chen, W.; Wong, M. W.; Gonzalez, C.; Pople, J. A. *Gaussian 03*, Revision B.03; Gaussian, Inc.: Wallingford, CT, 2004.